



Performance enhancement of direct ethanol fuel cell using Nafion composites with high volume fraction of titania



B.R. Matos^{*}, R.A. Isidoro, E.I. Santiago, F.C. Fonseca

Instituto de Pesquisas Energéticas e Nucleares, IPEN-CNEN, Avenida Prof. Lineu Prestes, 2242, São Paulo, SP 05508000, Brazil

HIGHLIGHTS

- A boost of DEFC performance at $T = 130$ °C using Nafion with 25 vol% of titania.
- OCV increase occurs at high fractions of inorganic phase in Nafion hybrids.
- Ethanol uptake hindered by high fractions of titania in Nafion hybrids.
- Proton conductivity at high temperatures weakly dependent on titania fraction.

ARTICLE INFO

Article history:

Received 6 March 2014

Received in revised form

18 June 2014

Accepted 18 June 2014

Available online 25 June 2014

Keywords:

Direct ethanol fuel cell

Nafion

Composite

Proton conductivity

Ethanol crossover

ABSTRACT

The present study reports on the performance enhancement of direct ethanol fuel cell (DEFC) at 130 °C with Nafion-titania composite electrolytes prepared by sol–gel technique and containing high volume fractions of the ceramic phase. It is found that for high volume fractions of titania (>10 vol%) the ethanol uptake of composites is largely reduced while the proton conductivity at high-temperatures is weakly dependent on the titania content. Such tradeoff between alcohol uptake and conductivity resulted in a boost of DEFC performance at high temperatures using Nafion-titania composites with high fraction of the inorganic phase.

© 2014 Elsevier B.V. All rights reserved.

1. Introduction

Nafion based composites, such as Nafion-titania (NT), are considered promising electrolytes for direct alcohol fuel cell (DAFC) applications at high temperatures ($T \sim 80$ – 130 °C) [1,2]. However, Nafion membranes swell dramatically in the presence of alcohol molecules that have a plasticizing effect on the polymer chains, thereby reducing the ionomer mechanical strength [3,4]. Moreover, the high alcohol permeability of Nafion allows the easy diffusion of ethanol molecules from the anode to cathode, which decreases in more than ~40% the DAFC efficiency [2,5]. The inorganic particles dispersed in the ionomeric matrix reduce the diffusion coefficient of alcohol molecules thereby reducing the polarization losses caused mainly by the cathodic fuel oxidation [5,6]. Nonetheless, previous reports showed that the alcohol molecules permeate

mostly through the Nafion ionic aggregates [4,6,7]. In this way, the synthesis of inorganic nanoparticles into Nafion ionic aggregates can minimize the diffusion of alcohol inside the composite electrolyte. One of the main challenges to reduce the alcohol crossover inside the electrolyte is to produce composite membranes with a high inorganic phase content preferentially localized inside Nafion hydrophilic domains [8–10]. In this context, the sol–gel synthesis has been reported as an efficient method to use Nafion's ionic aggregates as a template for the *in situ* incorporation of inorganic nanoparticles into the ionomer [9,11].

It is important to mention that most of the studies reporting on Nafion-based composites investigate rather low volume fraction of the inorganic phase [12–14]. This characteristic is possibly related to the rapid decrease of the proton conductivity of Nafion-oxide composites with increasing phase content of the low conductivity inorganic filler [15,16]. Indeed, the typical proton conductivity of oxide particles ($\sigma \sim 10^{-4}$ S cm⁻¹), usually associated with surface diffusion, is considerably lower than that of Nafion ($\sigma \sim 10^{-1}$ S cm⁻¹), which is governed by the molecular dynamics of

^{*} Corresponding author. Tel./fax: +55 11 3133 9282.

E-mail addresses: brmatos@usp.br, brunuss@gmail.com (B.R. Matos).

water [17,18]. Nonetheless, the DAFC performance was showed to increase substantially with the addition of small volume fractions (usually <10 vol%) of the inorganic particles into the ionomer matrix [12–14]. At $T = 130\text{ }^\circ\text{C}$, the current density at $\sim 400\text{ mV}$ of direct methanol fuel cells (DMFC) using Nafion-SiO₂ (3 wt%) was $\sim 0.6\text{ A cm}^{-2}$, while the current density obtained for Nafion at the same conditions was $\sim 0.3\text{ A cm}^{-2}$ [12]. Similarly, the power density of DMFC at $T = 145\text{ }^\circ\text{C}$ using Nafion-SiO₂ (3 wt%), Nafion-ZrO₂ (3 wt%), and Nafion-Al₂O₃ (3 wt%) were $\sim 350\text{ mW cm}^{-2}$, $\sim 300\text{ mW cm}^{-2}$, and $\sim 220\text{ mW cm}^{-2}$, respectively [12,13].

It is worth noting that direct ethanol fuel cell (DEFC) tests using composite membranes were seldom reported [14,19]. The performance of DEFC is substantially reduced as compared to DMFC due to the energy required to disrupt the C–C bond in the ethanol molecule, which usually results in a sluggish ethanol oxidation reaction. For example, the DEFC performance at $T = 120\text{ }^\circ\text{C}$ using Pt:Sn electrocatalysts and Nafion (thickness = 200–220 μm) is 0.02 A cm^{-2} ($\sim 600\text{ mV}$) [20]. Similarly to DMFC, the use of Nafion-titania composites with low volume fraction (<10 vol%) increased the performance of DEFC at $T = 130\text{ }^\circ\text{C}$ from $\sim 80\text{ mW cm}^{-2}$ (using N117) to $\sim 120\text{ mW cm}^{-2}$ (using Nafion-3wt% Silica) [19].

However, despite the considerable number of studies reporting on the improvement of DAFC performance by using Nafion-based composite electrolytes, the main composite properties promoting the increase of efficiency at high T are not fully understood [6]. The improved performance of DAFCs at high temperatures using Nafion-based composite electrolytes was mainly attributed to both the improved water retention properties of the inorganic phase and the reduced alcohol crossover through the electrolyte [12,13]. One of the central tenets of using Nafion-oxide composites for DAFC concerns the creation of new conducting pathways for proton diffusion through the few layers of water molecules existing at the surface of the inorganic phase at high temperatures [1]. Nonetheless, the volume fractions of oxide nanoparticles usually employed are far below the percolation threshold ($\sim 15\text{ vol}\%$). Thus, such low volume fractions indicate that there is no connectivity between the water molecules adsorbed at the surface of the dispersed oxide hindering possible charge transport contributions from the inorganic phase. In addition, such low dispersions of the inorganic phase are ineffective as a physical barrier to promote a significant reduction of the alcohol crossover. Thus, it is likely that the usually observed DAFC performance gain is not exclusively linked to the water sorption/retention capacity and reduced alcohol crossover.

More recent studies showed that Nafion-oxide composites with a high load of inorganic particles ($\sim 20\text{--}40\text{ wt}\%$) are bestowed with improved thermomechanical properties and lower alcohol permeability with respect to Nafion membranes [21,22]. Despite such interesting properties, investigations on high temperature DAFC tests using Nafion-based composites with high inorganic load are rarely found.

Herein a boost of DEFC performance at $T = 130\text{ }^\circ\text{C}$ using Nafion-titania with a high volume fractions (>10 vol%) of anatase titania produced by a sol–gel route is reported [10,11]. Such a result was possible due to both modifications of the sol–gel synthesis to allow the *in situ* incorporation of high volume fractions of well-crystallized stable nanoparticles in the ionic aggregates of Nafion, which promoted a reduction of the ethanol crossover, and to a detailed characterization of the electrical properties of composites at high temperatures.

2. Experimental

Commercial Nafion membranes (N115) were obtained from Dupont. Nafion 115 samples ($4 \times 5\text{ cm}^2$) underwent the standard procedure for cleaning and protonic activation [11] with successive

washing steps immersing the membranes in HNO₃ (7 mol L⁻¹), H₂O₂ (3 vol%), e H₂SO₄ (0.5 mol L⁻¹) at 80 °C for 1 h, with intermediate washing steps with deionized water (>15 M Ω , Millipore).

Titania (anatase) nanoparticles ($\sim 4\text{--}6\text{ nm}$ of diameter [11]) were synthesized *in situ* into N115 by the sol–gel technique with nominal volumetric concentrations $v = 10, 15, 20$ e $25\text{ vol}\%$ [10,11]. The synthesis of Nafion-titania composites NT_v consists basically in swelling the N115 in ethanol solvent for 1 h at room temperature RT to allow the easy access of titania precursor (titanium tetraisopropoxide/Ti(OR)₄ – 1 mol L⁻¹, Aldrich). Next, a peptizing agent is added to solution that promotes the controlled hydrolysis and condensation of the nanoparticles. These initial steps are performed under dry conditions to prevent hydrolysis in humid atmosphere. The titania formation is promoted by the addition of hydrogen peroxide (30 vol%) to the solution in the ratio 6.5:1 (H₂O₂:Ti(OR)₄). The condensation (crystallization) is carried out in an oven at 70 °C for 24 h. After the synthesis, the composite samples are washed in H₂SO₄ (0.5 mol L⁻¹) for 1 h followed by two successive washing steps with deionized water. Following the described procedure samples with final volume fractions $v = 11.1$ and $16.7\text{ vol}\%$ were obtained. The NT composites with higher volume fractions $v = 21.6$ and $26.4\text{ vol}\%$ are obtained by repeating the sol–gel synthesis procedure.

The mass uptake (W_u) of water and ethanol was estimated from the relative content of water, or ethanol, with respect to the dry sample. Samples were previously dried at 110 °C for 3 h. The volume uptake (V_u) was estimated using the following relations:

$$V_u = \frac{\Delta V}{(1 + \Delta V)} \times 100, \quad (1)$$

$$\Delta V = \frac{\rho_N(m_w - m_N)}{\rho_w m_N}, \quad (2)$$

where m_w and m_N are the wet and dry mass of the sample, respectively; ρ_N and ρ_w are the densities of dry Nafion and of the solvent, respectively; and ΔV is the ratio between the volume of the absorbed water to the volume of the dry polymer. The same procedure was used to estimate the volume fraction of the titania particles in Nafion membranes using the following equation:

$$\Delta V = \frac{\rho_N(m_T - m_N)}{\rho_T m_N}, \quad (3)$$

where m_T is the mass of the dry NT sample; ρ_T is the density of titania.

The water uptake as a function of temperature was obtained by using the air-tight humidity chamber used for the conductivity measurements at $RH = 100\%$. A hydrated Nafion membrane was positioned in the chamber and progressively heated in the temperature interval 100–180 °C with 10 °C steps. After two hours of stabilization at each temperature plateau, the chamber was opened and the membrane was removed for water uptake measurements.

Transmission electron microscopy (TEM) images were taken using a JEOL-2100F instrument with 200 kV of applied voltage on thin films (<100 nm) prepared with an ultramicrotome in the plane direction of the film.

Impedance spectroscopy (IS) data of NT composites were collected in a specially designed air-tight sample holder able to measure the proton conductivity in the range $T = 30\text{--}200\text{ }^\circ\text{C}$ with $RH = 100\%$ [23]. Nafion samples ($1.5 \times 1.5\text{ cm}^2$) were sandwiched between stainless steel spring-load contact terminals, which are insulated from the chamber walls. Circular contact pads of carbon cloth (1 cm diameter), with carbon ink (Teflon + Vulcan XC72) manually painted in both sides, were placed between stainless steel

contact terminals and the sample to facilitate water equilibration and improve the electrical contact. Prior to IS measurements, the sample was stabilized with water vapor for 24 h at 30 °C ($RH = 100\%$). A Solartron 1260 frequency response analyzer was used for IS measurements in the 4 mHz–3 MHz frequency (f) range with 100 mV applied amplitude. Parasitic resistances associated with the electrode-membrane interfaces were subtracted from the IS data to obtain accurate proton conductivity magnitude and activation energies [23]. Further details of IS measurement are described elsewhere [23]. The resistance of the samples was obtained from the intercept of the impedance semicircle at high frequencies ($f \sim 10^6$ Hz) with the real axis of the complex plane [23].

Nafion and composite membranes were evaluated in 5 cm² single fuel cells. The anode was prepared with PtSn/C (Pt:Sn 75:25 Basf) and Nafion loadings of 1.0 mg cm⁻² and 30 wt%, respectively. The cathode is composed of Pt/C and Nafion loadings of 1.0 mg cm⁻² and 30 wt%, respectively. The thicknesses of the hydrated membranes were ~160 μm, ~175 μm, ~180 μm, ~182 μm for Nafion, NT15, NT20 and NT25, respectively. The single cell was fed with 1.0 mol L⁻¹ ethanol solution and 5.0 mL min⁻¹ flux at the anode at 1 atm and with pure oxygen at the cathode at 3 atm absolute pressure. Fuel cell and oxygen humidifier temperatures were varied from 80 °C to 130 °C and polarization curves were obtained in duplicate experiments with estimated error of ~10% between 80 °C and 130 °C.

3. Results and discussion

Fig. 1 shows representative TEM images of NT15 composite. The low magnification image (Fig. 1(a)) obtained for NT composite shows a homogeneous distribution of titania nanoparticles. Typical interparticle distances range from ~9 nm to 12 nm, as observed in Fig. 1(b). High-resolution images (Fig. 1(c)) revealed crystalline anatase particles with estimated diameter of ~6 nm, in good agreement with both the crystallite size and the typical correlation distance previously estimated by both XRD and small angle X-ray scattering (SAXS), respectively [10].

Fig. 2 shows the water and ethanol uptake dependencies on the titania volume fraction (v) for NT composites.

It is observed in Fig. 2 that increasing v results in a significant decrease of both water and ethanol uptakes. Nevertheless, ethanol uptake is considerably more reduced and a twofold decrease, from ~60 to 30%, is observed when titania content increases from $v = 0$ to ~25 vol%. Previous SAXS revealed that titania nanoparticles added into Nafion matrix by the sol-gel technique are preferentially located in the hydrophilic phase [11]. Despite the reduction of the water uptake for NT composites, the composite with the highest content of the inorganic phase (NT25) absorbs a significant water

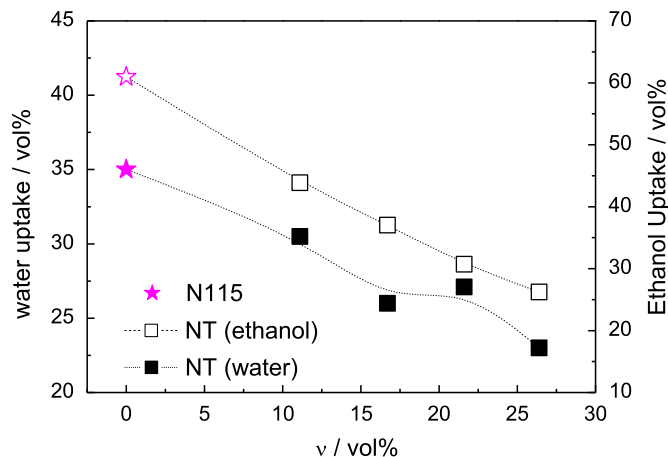


Fig. 2. Water and ethanol uptake of Nafion and Nafion-titania composites as a function of the inorganic phase volume fraction.

volume fraction (~22 vol%). Moreover, the percolation threshold of water for extrinsic proton conduction in the hydrophilic phase of Nafion is ~10 vol% [25]. Such value suggests that even at high volume fractions of titania the measured water uptake (>22%) allows for the water percolation in the polymer matrix. This feature indicates that titania particles did not disrupt the conduction pathways for proton diffusion in Nafion [25].

Fig. 3 shows the temperature dependence of water uptake of N115 and NT20. The water uptake of N115 is nearly constant in the ~40–100 °C range and increases appreciably with further increasing T , in good agreement with previous reports [27,28]. It is interesting to mention that the ethanol uptake was reported to exhibit a similar thermal dependence with respect to the water uptake displaying a pronounced increase of the ethanol absorption at $T > 100$ °C [28]. The polymer sample expands pronouncedly upon heating attaining ~83 vol% of aqueous phase at $T = 180$ °C evidencing a disentanglement of the ionomer chains followed by dissolution of the polymer membrane upon further increasing T [28]. Thus, at typical operating conditions of high-temperature polymer electrolyte fuel cells ($T \sim 130$ °C and $RH = 100\%$), unmodified Nafion membrane exhibits a pronounced increase of water content, which suggests a possible loss of the structural integrity that can affect the fuel cell performance.

NT20 composite absorbs half as much of the water absorbed by N115 in the entire temperature range. In addition, the NT20 water uptake is independent of the temperature increment up to $T \sim 130$ °C. Such a feature can result in a higher thermal and mechanical stability at high T , which is in good accordance with previous dynamic

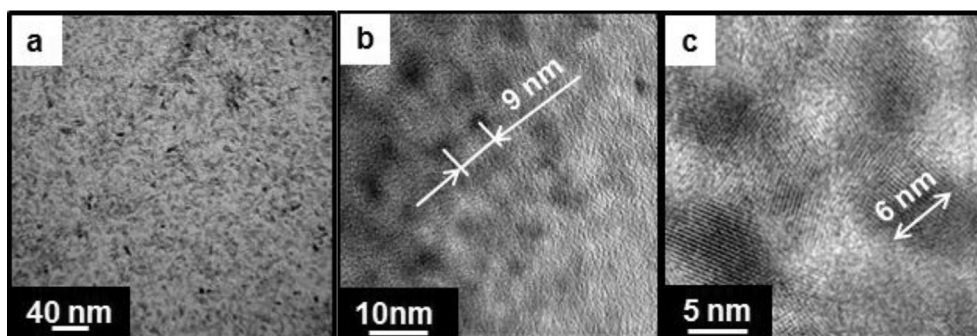


Fig. 1. TEM images of the Nafion-titania containing 15 vol% of the inorganic phase (a) low-magnification image, (b) high-magnification with typical interparticle distance marked, (c) high-resolution image of the anatase nanoparticles.

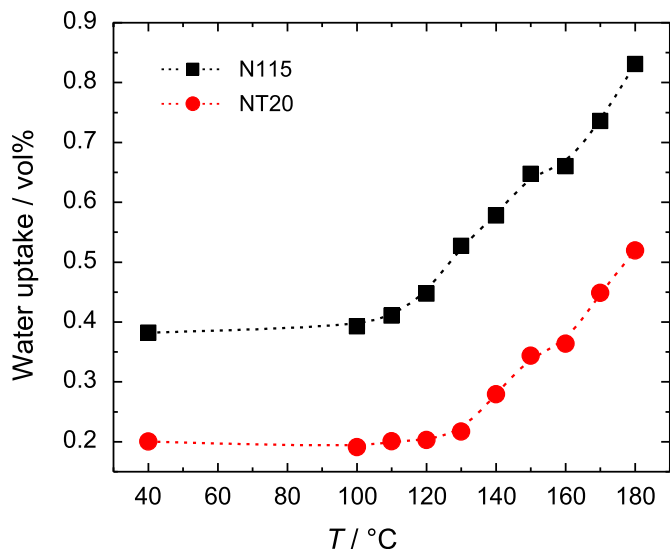


Fig. 3. Temperature dependence of water uptake for Nafion and Nafion-titania with 20 vol% of inorganic phase.

mechanic analysis (DMA) of NT composites [10,24]. The higher stability of NT composites is an important property for maintaining the DEFC performance at high T and RH [11].

Fig. 4 shows Arrhenius plots for the proton conductivity of N115 and NT composites at $RH = 100\%$.

The proton conductivity dependence on the temperature for N115 can be separated into two regimes: one occurring from ~ 30 to 90 °C with an Arrhenius-like behavior, followed by a non-Arrhenius thermal dependence for $T > 90$ °C [16,23]. At low temperature, increasing the titania content from $v = 10$ to 20 vol% resulted in an abrupt decrease of the proton conductivity at $T = 40$ °C from $\sigma \sim 0.025$ S cm $^{-1}$ to 0.009 S cm $^{-1}$, respectively. This result is in good accordance with previous proton conductivity studies of Nafion-based composites in which a decrease of σ with increasing oxide content is observed even at low $v < 10$ vol% [11]. Such an abrupt decrease of σ can be linked to the reduced amount of water

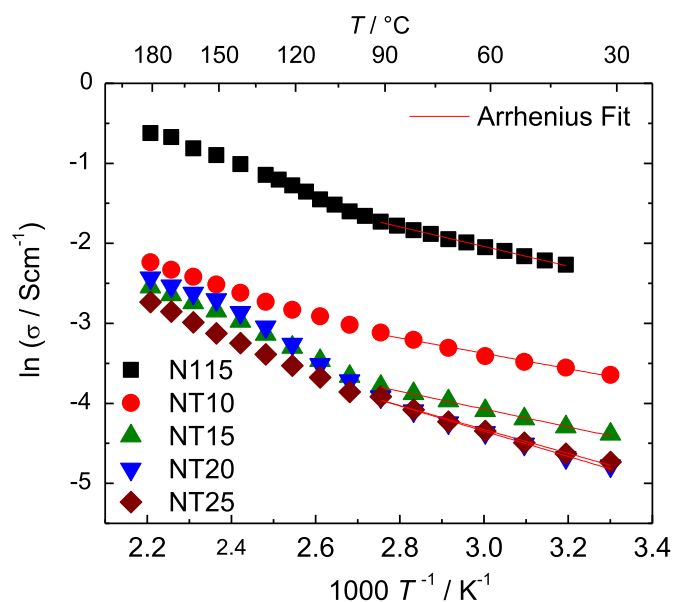


Fig. 4. Arrhenius plots for proton conductivity of Nafion and Nafion-titania composites at $RH = 100\%$.

absorbed and an increased volume fraction of the less conducting phase in the composite samples [1]. However, it is interesting to note that for $T > 130$ °C the proton conductivity has a weak dependence on the inorganic phase volume fraction and composite samples exhibit much closer σ values. Such a relatively high conductivity at high temperature is not straightforward and can be related to different features. At high temperature and high relative humidity it is expected that the proton transport is essentially controlled by the molecular dynamics of water. Such a feature, along with increased water absorption at high temperature, can reduce the influence of the inorganic phase on the proton transport. Table 1 shows the proton conductivity values for NT composites at $T = 40$ °C and $T = 130$ °C and the apparent activation energy (E_a) of the Arrhenius-like dependence of the proton conductivity in the range $T \sim 30$ – 90 °C.

The activation energy increases with increasing titania from $v = 10$ to 20 vol% and for further increase of the inorganic phase (NT25) the activation energy is not significantly altered. The proton conduction in aqueous media in perfluorosulfonate ionomers takes place via structural diffusion and vehicular mechanism [26]. At low temperatures ($T < 80$ °C) and high relative humidity the proton diffusion occurs mostly by structural diffusion, which defines the characteristic activation energy of $E_a \sim 0.10$ eV for Nafion membranes in the range $T \sim 30$ – 90 °C [23,26]. The higher activation energies observed for Nafion-titania composites with 20 and 25 vol% suggest that the proton diffusion has a higher contribution from the vehicular mechanism [17,26]. The large content of nanoparticles possibly increases the fraction of less mobile water molecules and, consequently, decreases the amount of bulky water that favors the proton conduction via structural diffusion [26]. Such lower contribution of structural diffusion in high- v NT composites is probably associated with an increased vehicular transport. At high filler volume fractions there is a closer proximity between inorganic nanoparticles that allows the connectivity of adsorbed water molecules providing new pathways for vehicular proton conduction in composite membranes.

It is worth noting that the proton conductivities of N115 and NT composites follow a non-Arrhenius thermal dependence for $T > 90$ °C. Although the proton conductivity dependence on temperature for N115 follows the Vogel–Tamman–Fulcher (VTF) empirical law, there is no consensus so far whether this thermal dependence is associated with the increase of the proton conductivity above the polymer glass transition, or related to the irreversible polymer expansion upon water sorption [23]. The results of Figs. 3 and 4 for the composites suggest that proton conductivity has a weak dependence on the water uptake at high T , a feature more marked between $T \sim 90$ °C and ~ 130 °C for composite samples. The water uptake for NT20 composite is nearly constant up to $T \sim 130$ °C, whereas the proton conductivity shows a behavior similar to Nafion in which the deviation from Arrhenius behavior is evident for $T > 90$ °C.

The combined results of Figs. 3 and 4 show that NT composites with high titania content have low ethanol uptake and reasonable proton conductivity, thus are promising candidates for DEFC

Table 1

Proton conductivity of Nafion-titania composites at $T = 40$ °C and $T = 130$ °C and the calculated activation energy in the range $T \sim 30$ – 90 °C.

Sample	$\sigma_{40\text{ °C}}$ [S cm $^{-1}$]	$\sigma_{130\text{ °C}}$ [S cm $^{-1}$]	E_a [eV]
N-115	0.104	0.319	0.10
NT10	0.029	0.066	0.08
NT15	0.014	0.044	0.09
NT20	0.009	0.048	0.13
NT25	0.009	0.034	0.13

electrolytes at high T . The effect of titania content on the performance of DEFCs using NT electrolytes was studied by I – V curves, as shown in Fig. 5.

Fig. 5 shows the power density (p) and polarization (I – V) curves of DEFC as a function of temperature for Nafion (a and b) and for Nafion-titania composites containing 15 vol% (c and d); 20 vol% (e and f)

and 25 vol% (g and h). The polarization (I – V) curves obtained in the range $T \sim 80$ – 130 °C evidenced typical features of DEFC: i) a large drop of the open circuit voltage (OCV) with respect to the theoretical equilibrium potential for ethanol electro-oxidation ($V_{\text{eq}} \sim 1.145 \text{ V}/T = 25$ °C) and ii) a large polarization loss at low current densities due to activation polarization [5,6]. The OCV drop

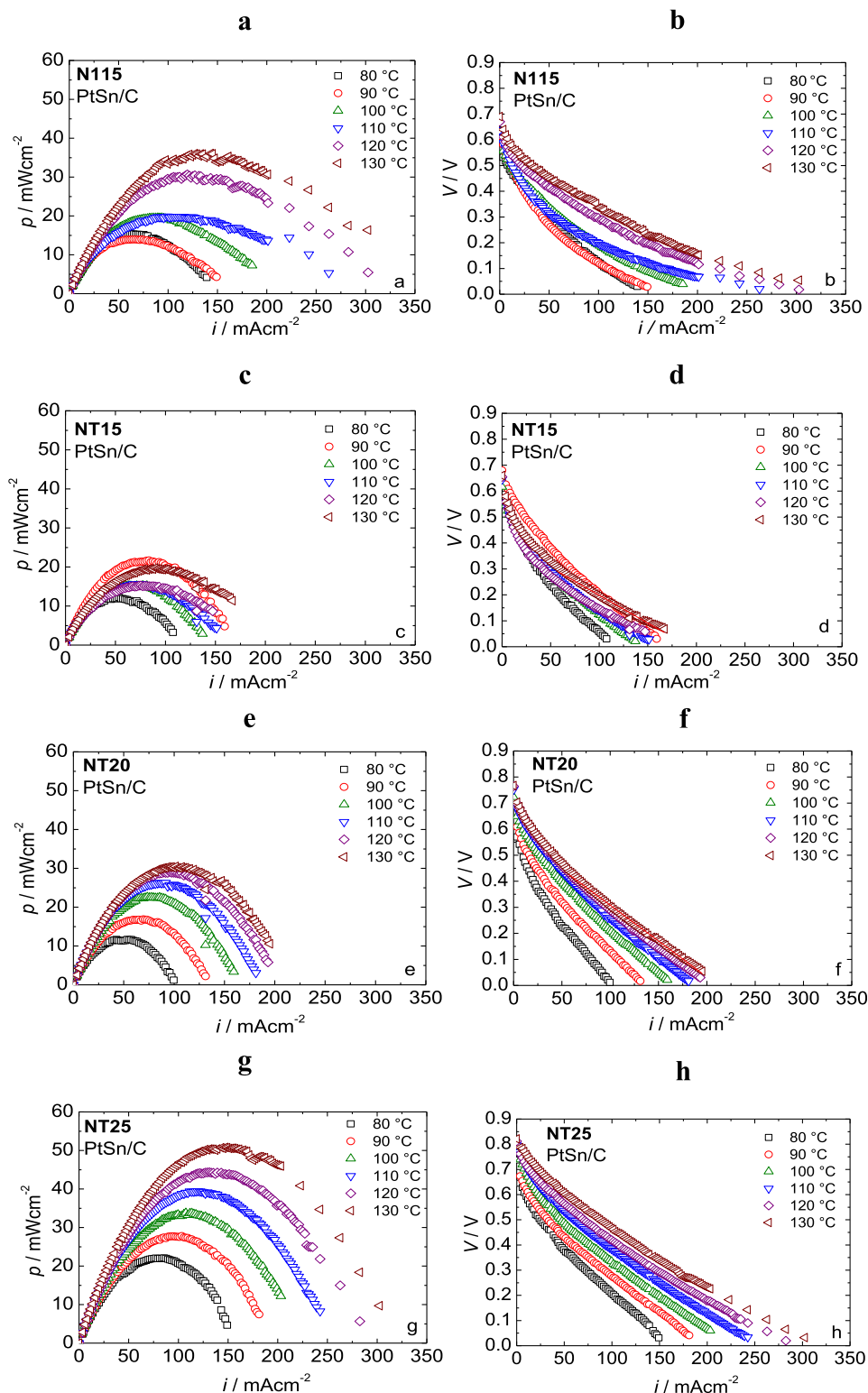


Fig. 5. Power density (p) and polarization (I – V) curves of DEFC as a function of temperature for Nafion (a and b) and for Nafion-titania composites containing 15 vol% (c and d); 20 vol% (e and f); and 25 vol% (g and h).

is usually attributed to the crossover of ethanol molecules from the anode to the cathode whereas the activation polarization is attributed to the sluggish ethanol oxidation reaction [5]. Thus, taking into account that the studied fuel cells have nominally identical electrodes, the differences observed in the polarization curves, markedly at high current densities, are essentially related to the properties of the investigated electrolytes [10]. It can be observed that increasing T increases the DEFC performance in the entire temperature range investigated. Moreover, the ohmic drop is higher for NT composites than for N115. The calculated specific resistances from the linear portion of I – V curves at $T = 130$ °C for N115, NT15, NT20 and NT25 are $\sim 1.5 \Omega \text{ cm}^{-2}$, $\sim 2.1 \Omega \text{ cm}^{-2}$, $\sim 2.7 \Omega \text{ cm}^{-2}$, $\sim 2.1 \Omega \text{ cm}^{-2}$, respectively. Both the increase of the DEFC performance with increasing T and the ohmic drop inferred from the polarization curves are in good agreement with the temperature dependence of the proton conductivity of the composite electrolytes (Table 1 and Fig. 4).

It can be inferred from Fig. 5 that the open circuit voltage (OCV) of the DEFC using NT composites increases with increasing the titania volume fraction. At $T = 130$ °C the OCV increases in the following order: NT15 (~ 0.66 V) < Nafion 115 (~ 0.69 V) < NT20 (~ 0.77 V) < NT25 (~ 0.82 V). The higher OCV for the fuel cell with NT25 electrolyte represents a gain of ~ 130 mV in the DEFC performance with respect to Nafion 115. As the OCV values are mainly associated with the ethanol crossover within the electrolyte, the increment of the OCV for DEFCs strongly indicates the decrease of the ethanol permeability in NT composites with high v , in good accordance with the lower ethanol uptake showed in Fig. 2.

It is interesting to note that by increasing the sample thickness the OCV values were reported to increase [29]. However, appreciable OCV increases (~ 0.516 V– 0.573 V) are observed with increasing the thickness of Nafion from $\sim 60 \mu\text{m}$ (Nafion 112) to $\sim 220 \mu\text{m}$ (Nafion 117). In the studied composites the increase of the membrane thickness ranges from $\sim 175 \mu\text{m}$ to $\sim 182 \mu\text{m}$ with increasing titania fraction. Such thickness variation is insignificant as compared to the necessary thickness increase to have appreciable changes in OCV in Nafion. Such feature indicates that the thickness of the composites cannot account for the increase of OCV values with increasing titania fraction.

The performance of DEFCs using NT15 and NT20 composites is lower than the one obtained for N115. It is interesting to mention that the performance of DEFC using NT15 composites with Pt electrocatalyst was reported to be higher than that of Nafion 115 [10]. The DEFC power density of N115 and NT15 with Pt electrocatalyst at $T = 130$ °C was $p \sim 12 \text{ mW cm}^{-2}$ and $\sim 15 \text{ mW cm}^{-2}$, respectively [10]. This result suggests that the performance of DEFCs using a poor electrocatalyst for ethanol oxidation reaction (such as Pt) is dominated by both the activation polarization and alcohol crossover, while the ohmic drop due to less conducting electrolyte is not as relevant. On the other hand, the polarization curves of DEFC using NT15 and Pt/Sn electrocatalyst (Fig. 5) show that as the activation polarization loss decreases by using a more active electrocatalyst, the ohmic drop has a major contribution to the performance of DEFCs. Thus, the low conductivity of NT15 and NT20 with respect to Nafion 115 (Fig. 4) results in higher ohmic drops in I – V curves that decrease the DEFC performance. However, as shown in Fig. 5, the DEFC performance increases with increasing titania volume fraction in NT composites regardless the increased ohmic drop due to the inorganic phase. Interestingly, the DEFC using NT25 electrolyte has the highest maximum power density ($p \sim 50 \text{ mW cm}^{-2}$) at 130 °C, surpassing the one observed for N115. This result demonstrates that the tradeoff between low ethanol uptake and relatively good proton conductivity at high temperature of NT composites (with high content of the oxide phase) contribute to increase the DEFC performance. However, the high ohmic drop of

NT25 indicated that the increased OCV plays an important role for the increased DEFC performance. Nevertheless, it is interesting to note that the increased power density of the NT25 sample cannot be exclusively ascribed by the 130 mV gain in OCV. Thus, it is possible that the reduced ethanol crossover contributes to decrease the mixed potential associated with cathodic ethanol oxidation [5,6]; however, more detailed electrochemical measurements would be necessary to quantitatively assess such a contribution.

4. Conclusion

The study of composites with high fractions of inorganic phase allowed for a clear understanding of the role played by oxide nanoparticles in Nafion composite electrolytes. The addition of high fractions of the inorganic phase by sol–gel synthesis into Nafion contributed to reduce the ethanol uptake while the proton conductivity at high temperatures was not significantly altered. The balance between these two properties of Nafion-titania composites reflected in a substantial increase of DEFC performance at high temperatures. The boost of DEFC efficiency using Nafion-titania composite electrolytes was associated with a lower ethanol uptake and a reduction of the cathodic ethanol oxidation.

Acknowledgment

Thanks are due to Prof. A.C. Tavares (TEM). Thanks are also due to the Brazilian funding agencies (CAPES, CNPQ, FAPESP-13/50151-5) and CNEN.

References

- [1] G. Alberti, M. Casciola, *Annu. Rev. Mater. Res.* 33 (2003) 129.
- [2] V. Baglio, A. Di Blasi, A.S. Arico, V. Antonucci, P.L. Antonucci, C. Trakanprapai, V. Esposito, S. Licocchia, E. Traversa, *J. Electrochem. Soc.* 152 (2005) A1373.
- [3] T. Kyu, A. Eisenberg, *J. Polym. Sci. Polym. Symp.* 71 (1984) 203–219.
- [4] S.K. Young, S.F. Trevino, N.C. Beck Tan, *J. Polym. Sci. B Polym. Phys.* 40 (2002) 387.
- [5] J.J. Linares, T.A. Rocha, S. Zignani, V.A. Paganin, E.R. Gonzalez, *Int. J. Hydrogen Energy* 38 (2013) 620–630.
- [6] N.W. Deluca, Y.A. Elabd, *J. Polym. Sci. B Polym. Phys.* 44 (2006) 2201.
- [7] B. Loppinet, G. Gebel, C.E. Williams, *J. Phys. Chem. B* 101 (1997) 1884.
- [8] D. Truffier-Boutry, A. De Geyer, L. Guetaz, O. Diat, G. Gebel, *Macromolecules* 40 (2007) 8259.
- [9] K.A. Mauritz, M.K. Hassan, *Polym. Rev.* 47 (2007) 543.
- [10] B.R. Matos, R.A. Isidoro, E.I. Santiago, M. Linardi, A.S. Ferlauto, Ana C. Tavares, Fabio C. Fonseca, *J. Phys. Chem. C* 117 (2013) 16863–16870.
- [11] E.I. Santiago, R.A. Isidoro, M.A. Dresch, B.R. Matos, M. Linardi, F.C. Fonseca, *Electrochim. Acta* 54 (2009) 4111.
- [12] A.S. Arico, V. Baglio, A. Di Blasi, P. Creti, P.L. Antonucci, V. Antonucci, *Solid State Ionics* 161 (2003) 251.
- [13] V. Baglio, A.S. Arico, V. Antonucci, I. Nicotera, C. Oliviero, L. Coppola, P.L. Antonucci, *J. Power Sources* 163 (2006) 52.
- [14] R.A. Isidoro, B.R. Matos, M.A. Dresch, E.V. Spinacé, M. Linardi, E. Traversa, F.C. Fonseca, E.I. Santiago, *ECS Trans.* 25 (2009) 757.
- [15] B.R. Matos, E.I. Santiago, J.F.Q. Rey, A.S. Ferlauto, E. Traversa, M. Linardi, F.C. Fonseca, *J. Power Sources* 196 (2011) 1061.
- [16] V. Di Noto, R. Gliubbizzi, E. Negro, G. Pace, *J. Phys. Chem. B* 110 (2006) 24972.
- [17] S. Raz, K. Sasaki, J. Maier, I. Riess, *Solid State Ionics* 143 (2001) 181.
- [18] K.-D. Kreuer, *Chem. Mater.* 8 (1996) 610–641.
- [19] A. Di Blasi, V. Baglio, A. Stassi, C. D'Urso, V. Antonucci, A.S. Arico, *ECS Trans.* 3 (2006) 1317.
- [20] J. Mann, N. Yao, A.B. Bocarsl, *Langmuir* 22 (2006) 10432.
- [21] M. Casciola, D. Capitani, A. Comite, A. Donnadio, V. Frittella, M. Pica, M. Sganappa, A. Varzi, *Fuel Cells* 8 (2008) 217.
- [22] M. Casciola, G. Bagnasco, D. Capitani, A. Donnadio, L. Micoli, M. Pica, M. Sganappa, M.A. Turco, *Fuel Cells* 9 (2009) 394.
- [23] B.R. Matos, C.A. Andrade, E.I. Santiago, R. Muccillo, F.C. Fonseca, *Appl. Phys. Lett.* 104 (2014) 091904.
- [24] B.R. Matos, E.M. Arico, M. Linardi, A.S. Ferlauto, F.C. Fonseca, *J. Therm. Anal. Calorim.* 97 (2009) 591.
- [25] W.Y. Hsu, J.R. Barkley, P. Meakin, *Macromolecules* 13 (1980) 198–200.
- [26] K.-D. Kreuer, M. Schuster, B. Obliers, O. Diat, U. Traub, A. Fuchs, U. Klock, S.J. Paddison, J. Maier, *J. Power Sources* 178 (2008) 499–509.
- [27] K.-D. Kreuer, *Solid State Ionics* 252 (2013) 93.
- [28] G. Gebel, P. Aldebertt, M. Pineri, *Polymer* 34 (1993) 333.
- [29] J.G. Liu, T.S. Zhao, Z.X. Liang, R. Chen, *J. Power Sources* 153 (2006) 61–67.